
A hybrid-excited flux-switching machine for fault short-circuit current limitation in embedded DC alternator applications

Andre Nasr¹, Sami Hlioui², Mohamed Gabsi¹

1. SATIE, ENS Paris-Saclay, universit  Paris-Sud, CNRS, universit  Paris-Saclay
61 avenue du Pr sident Wilson, 94325 Cachan, France

anasr@satie.ens-cachan.fr, mohamed.gabsi@ens-cachan.fr

2. SATIE, CNAM, ENS Paris-Saclay, CNRS
292 rue St Martin, 75141 Paris, France

sami.hlioui@satie.ens-cachan.fr

ABSTRACT. This paper presents a new design of a Hybrid-Excited Flux Switching Machine (HEFSM) proposed for DC power generation in embedded applications. Unlike classical hybrid-excited machines, the HEFSM has a low remanent flux-linkage making its characteristics similar to those of a wound field-machine. We will discuss in the first section the advantages of such characteristics in critical applications. Later on, we will present the design of the HEFSM and we will determine its electromagnetic performances using a finite element method before carrying out a study on its short-circuit current limitation capability in faulty conditions. It has been shown that the HEFSM can be easily demagnetized by simply cutting off the excitation current. This makes it suitable for critical applications like aircraft power generation.

R SUM . Cet article pr sente une nouvelle structure d'une machine   commutation de flux   double excitation (MCFDE) d di e pour la g n ration embarqu e DC. Cette machine, et malgr  la pr sence d'aimants permanents, pr sente des caract ristiques semblables   une machine   excitation bobin e, surtout un flux r manent faible. Nous discutons dans la premi re partie les avantages de telles caract ristiques. Nous pr sentons dans la suite la structure de la MCFDE et nous d terminons ses performances  lectromagn tiques en utilisant un mod le en  l ments finis avant d' tudier sa capacit    limiter le courant de court-circuit dans des conditions de d faut. Il a  t  montr  que la MCFDE peut  tre d magn tis e en coupant le courant d'excitation. Ceci la rend adapt e aux applications critiques comme la g n ration avionique.

KEYWORDS: dc alternator, embedded applications, flux-switching machines, hybrid-excited machines, starter-generator.

MOTS-CL S : alternateur dc, applications embarqu es, machines   commutation de flux, machines   double excitation, alterno-d marreur.

DOI:10.3166/EJEE.18.361–384   2016 Lavoisier

1. Introduction

Hybrid-Excited machines allow to combine two excitation sources : permanent magnets and field coils. The permanent magnets form a primary excitation source that allows to generate torque with high efficiency as in Permanent Magnet (PM) machines. On the other side, the field coils act as a secondary excitation source offering a practical control of the excitation flux as in Wound-Field (WF) machines. Hybrid-excited machines allow then to inherently combine the advantages of the PM and WF machines in a single structure (Hlioui *et al.*, 2013).

Permanent magnet machines are widely used in electric and hybrid electric vehicles due to their high power density and high efficiency (Laskaris, Kladas, 2010; Zhang *et al.*, 2015). They involve low losses as they require no current to produce their excitation flux due to the presence of permanent magnets. This helps achieve compact designs that are suitable for embedded applications like automotive electric traction. However, since the air-gap flux in such machines is constant, vector control techniques are used in order to extend the working speed-range above the base speed limit. These techniques, also known as flux weakening, can cause high copper losses and a high demagnetization risk of the permanent magnets (Zhu, Cheng, 2005). Furthermore, in some cases such in wide-speed-range operation, the power electronics used to control the machine must be oversized which results in an increase of the overall costs (Ammar *et al.*, 2012). This problem mainly occurs when using PM machines with a low armature reactance. In such cases, a high current must be used in order to have enough armature reaction for flux weakening.

In recent years, Flux-Switching Permanent Magnet (FSPM) machines have gained increasing interest over conventional permanent magnet machines in embedded applications (Hoang *et al.*, 1997). The FSPM offers very good flux-weakening capabilities due to its high phase reactance (Hoang *et al.*, 2000). It has in theory a constant-power infinite-speed-range using a relatively low phase current. Furthermore, having the same rotor as a switched reluctance machine, the FSPM offers mechanical robustness at high rotational speeds. The presence of permanent magnets in the stator results in a simplified and more efficient cooling system which leads in return to a better control of the magnets temperature.

Most of the embedded applications nowadays require the use of the same electrical machine for both motor and generator modes (Cai, 2004). This solution helps reducing the weight and the space occupied by the traction and the generation system in comparison with other solutions using two different machines (Chau, Chan, 2007). In both modes, the machine is connected to a converter feeding or absorbing power from a DC bus. In generator mode, all permanent magnet machines including the FSPM require an active rectifier as shown in Figure 1. In this configuration, the rectifier is the only control parameter left for flux weakening or flux enhancing since the excitation flux of the PM machine is constant. However, in the case of a loss of power electronics, the non controlled permanent magnet machine can generate high voltages at high-speed operation points which imposes supplementary protection systems to

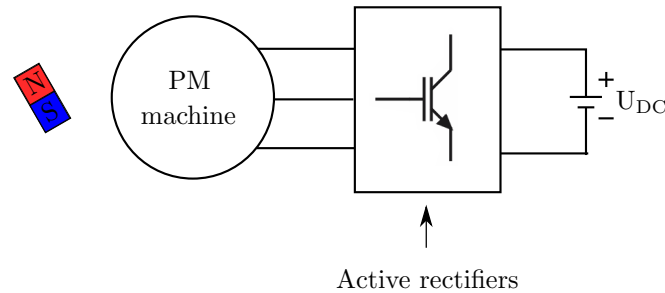


Figure 1. DC alternator configuration using a controlled converter

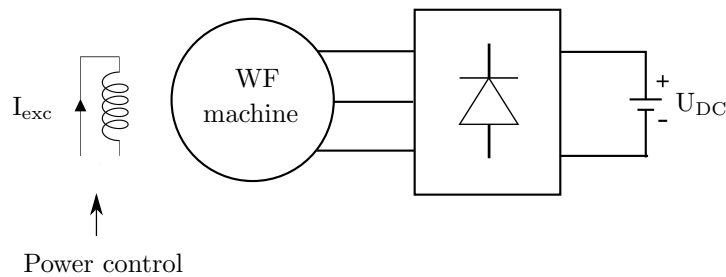


Figure 2. DC alternator configuration using a diode bridge rectifier

disconnect the machine from the network (Friedrich, Girardin, 2009). But in the case of a phase short-circuit, the high fault current can damage both the machine and the vehicle and cannot be cut-off until the machine stops rotating. For these reasons, PM machines are avoided in critical embedded applications like aircraft power generation and wound field machines are used instead. The excitation flux in a WF machine is generated by a controlled DC excitation current I_{exc} in the field coils and no permanent magnets are used. Therefore, it can be easily demagnetized to cancel all risks of high voltages in case of fault. Moreover, having a controlled excitation flux, a WF machine can be used in a DC alternator configuration using the more reliable diode bridge rectifier as shown in Figure 2.

The Wound Rotor Synchronous (WRS) machine is used in a broad range of applications including aircraft power generation. It offers a practical control of its excitation flux making it ideal for variable speed operation. It is also inherently safer comparing with PM machines because of its demagnetization capability. However, since the field coils are installed on the rotor, slip rings and brushes are usually used in order

to have electrical contact between the static and the rotating parts. In aircraft power generation, such structures are avoided and the WRS machine is usually included in a brushless design known as the three-stage machine (Raimondi *et al.*, 2002; Avery *et al.*, 2007). This machine uses a rotating diode bridge rectifier in order to avoid using slip rings and brushes in the WRS machine. This latter, and despite all its advantages (safety, flux control), has a low power density compared to PM machines which leads to power systems with more weight and more volume.

We will present in this paper a new design of a Hybrid-Excited Flux-Switching Machine (HEFSM) proposed for starter-generator applications in embedded systems. Despite having permanent magnets, this design has a low remanent flux-linkage due to its special stator structure which makes it suitable for future use in aircraft power systems. The HEFSM was studied by the authors in (Nasr *et al.*, 2017b). A 3 kW prototype was presented and an experimental investigation has been carried out in order to evaluate the electromagnetic and thermal performances of the machine. However, the prototype studied in that paper has a preliminary design and doesn't comply with the safety requirements for aircraft power generation. In (Nasr *et al.*, 2017a), authors have presented a design optimization methodology in order to fulfill these safety requirements. Comparisons between experimental results and simulations have been carried out in order to validate the finite element model used. The same model will be used in this paper to carry out the simulations (Ansys Maxwell, 2015). One of the optimized designs resulting from the optimization methodology was studied in (Nasr *et al.*, 2016). That paper has shown that it is possible for the HEFSM to comply with the safety requirements while having improved overall performances.

We will study in this paper the impact of some geometric and magnetic parameters of the HEFSM on its overall performances especially on its capacity to limit the short-circuit current. We will discuss at first the advantages of hybrid excitation especially in embedded DC systems. The different topologies of hybrid excited machines will be presented and compared to the HEFSM. Later on, a finite element model will be used to determine the electromagnetic performances in generator and motor mode. The short-circuit current limitation capability of the HEFSM will be discussed in the final section. Sensibility studies will be carried out to assess the impact of changing the width of the magnetic bridge of the machine and its permanent magnet remanent flux density on its overall performances.

2. The HEFSM : a hybrid-excited machine with low remanent flux

Hybrid-excited machines can be classified into many categories. One of these categories involves the way of how the two excitation sources magnetically combine. In **series hybrid excitation** machines, the flux generated by the field coils passes through the permanent magnets as shown in Figure 3. These machines have a limited flux regulation capability due to the big magnetic reluctance of the permanent magnet being in series with the magnetic circuit reluctance of the field coil. This hybrid excitation principle also increases the risk of PM demagnetization in case of flux weakening

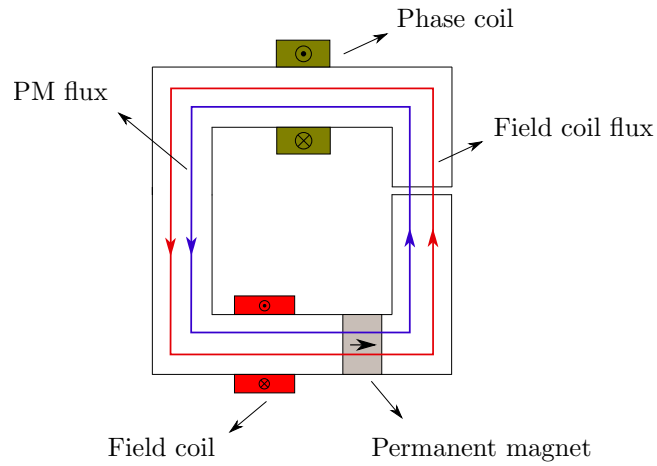


Figure 3. Series hybrid excitation principle

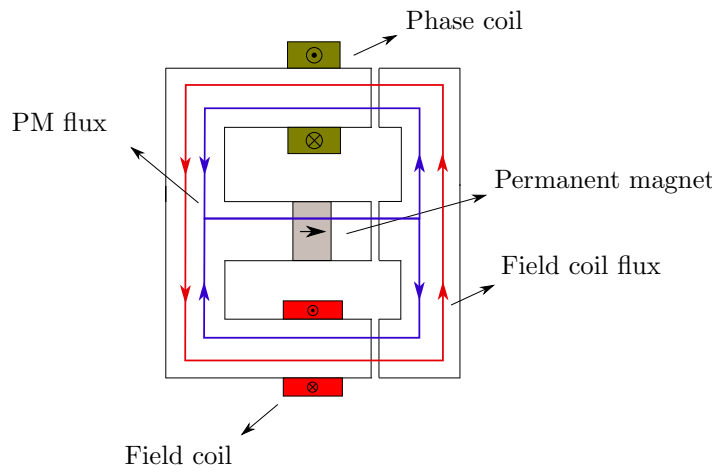


Figure 4. Parallel hybrid excitation principle

(Leonardi *et al.*, 1997). On the other hand, **parallel hybrid excitation** machines have a much lower risk of PM demagnetization. As Figure 4 shows, the flux created by the field coil does not pass through the permanent magnet. This configuration increases the flux regulation capability of the field coil. Another classification for hybrid-excited

machines involves the positioning of each of the excitation sources on the stator or on the rotor. Having the field coils positioned on the stator allows to have a brushless system with higher reliability. Having the permanent magnets positioned on the stator as well allows better heat dissipation and better control of their temperature. This also leads to a robust rotor suited for high rotational speeds.

Whatever the configuration used, a hybrid-excited machine allows to combine the advantages of permanent magnet machines and wound field machines : high power density, high efficiency and flux regulation capability (Amara *et al.*, 2009). These characteristics combined make it a very interesting machine for DC power systems used in embedded applications (Wang, Deng, 2012b). However, all the classical hybrid-excited machines that can be found in literature have a flux characteristic like the one shown in Figure 5. The remanent flux ϕ_0 in these machines is relatively high compared to the maximum flux value reached using the excitation current I_{exc} . This high value of ϕ_0 leads to a high remanent voltage at high speeds which is incompatible with the safety requirements mentioned above. These machines can be designed to have lower remanent flux ($\phi_0 - \Delta\phi$) but this will automatically reduce the maximum flux value reached.

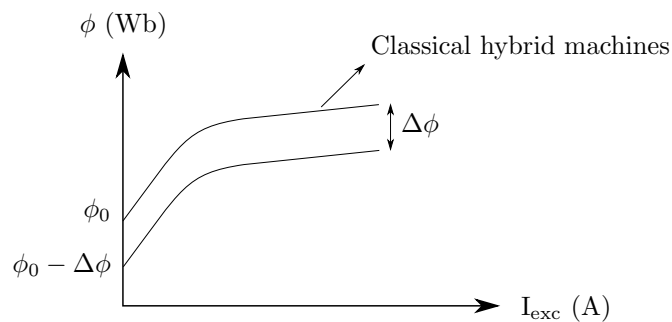


Figure 5. No-load flux-linkage characteristics in classical hybrid machines

In order to fulfill the requirement of having a low remanent flux, one can imagine a configuration like the one shown in Figure 6. We can notice that the flux generated by the permanent magnet passes through a magnetic circuit other than the one containing the phase coil. This alternative path has a smaller magnetic reluctance acting like a magnetic short-circuit. One of the machines having this configuration is the Hybrid-Excited Flux-Switching Machine (HEFSM) presented in Figure 7 (Nasr *et al.*, 2016; Hoang *et al.*, 2007). The magnetic short-circuit in this machine is accomplished by a magnetic bridge in the stator. This kind of structures have been studied in (Owen *et al.*, 2010; Wang, Deng, 2012a). Authors in these publications have examined the impact of the magnetic bridge on the flux control capability. It has been found that a larger magnetic bridge increases the effectiveness of the field coils. However, these studies

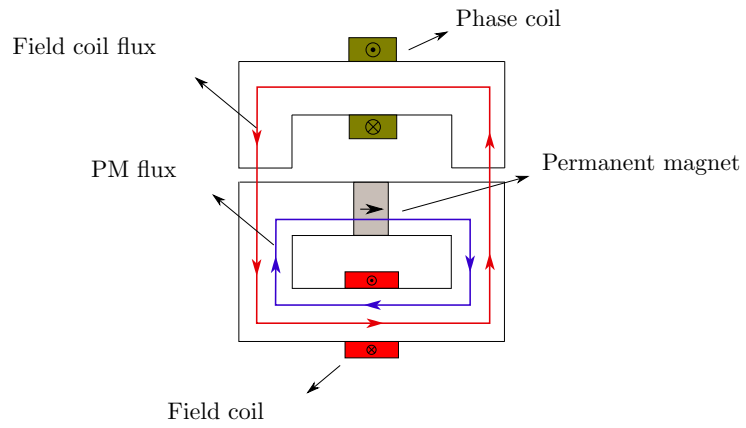


Figure 6. Hybrid excitation with low remanent flux-linkage

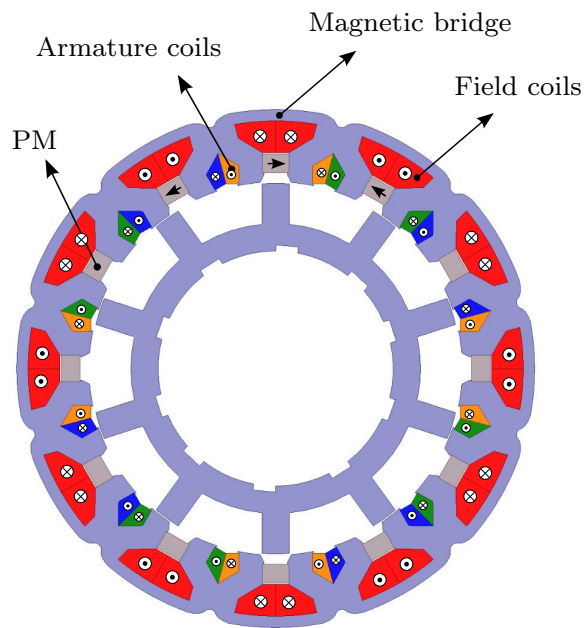


Figure 7. Hybrid-excited flux-switching machine

haven't dealt with the problem of having a low remanent flux and have presented machines with the same flux characteristic as in Figure 5 (classical machines). The design of a HEFSM having a low remanent flux has been considered in (Nasr *et al.*, 2017a). The authors of this paper have presented a design methodology allowing to maximize the electromagnetic performances in generator mode while limiting the remanent voltage to very low values. The same methodology has been used to design the machine in Figure 7.

We will present in the next section the electromagnetic performances of the HEFSM in no-load conditions, in generator mode and in motor mode. At first, we will present the no-load flux-linkage characteristic and we will analyse the magnetic behavior of the machine when no excitation current is used. Later on, we will determine the performances of the HEFSM in generator mode in a DC alternator configuration and in motor mode.

3. Electromagnetic performances of the HEFSM

The HEFSM studied in this paper (Figure 7) has a 10 poles rotor and a 12 poles stator both made of silicon-iron sheets (SiFe) (Figure 8). The stator is composed of 12 elementary cells each containing 2 teeth, 1 Samarium-Cobalt (SmCo) magnet, 1 armature coil and 1 slot for field coils (Table 1). Each phase is composed of 4 armature coils connected in series. Regarding the field winding, this structure contains 12 concentric coils positioned above armature coils in order to avoid overlapping.

Table 1. HEFSM specifications

Stator and rotor sheet material	SiFe
Number of stator elementary cells	12
Number of phases	3
Number of coils per phase	4
Number of turns per coil	26
SmCo PM residual induction	1 T (20 °C)
Coercivity of magnetic polarization	1400 kA/m (20 °C)
Number of rotor teeth	10
Active length	35 mm
External stator diameter	140 mm
Air gap	0.4 mm
Nominal power	3 kW
Nominal speed	12500 rpm

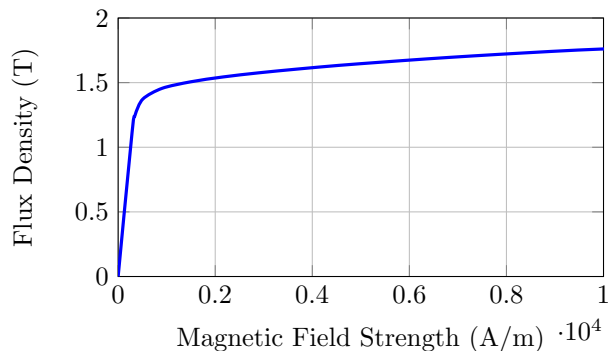


Figure 8. B-H magnetization characteristic for SiFe

3.1. No-load flux-linkage

The no-load flux-linkage of the HEFSM is presented in Figure 9 versus the excitation current density with and without permanent magnets. One can clearly see the contribution of the permanent magnets in reaching higher flux values. At $\delta_{exc} = 12.5 \text{ A/mm}^2$, the flux value reached with permanent magnets is about 45 % higher than without PMs (36.4 mWb instead of 25 mWb). However, at $\delta_{exc} = 0 \text{ A/mm}^2$, we can notice that the remanent flux-linkage is very low (1.47 mWb). The flux char-

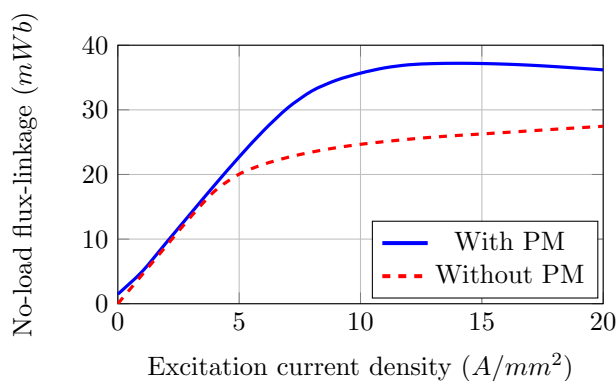


Figure 9. No-load flux-linkage in d-axis position with and without permanent magnets

acteristic of the HEFSM differs then from that of a classical hybrid-excited machine (Figure 5) and is closer to the one of a wound-field machine.

Figure 10 shows the flux lines and the flux density patterns at $\delta_{exc} = 0 \text{ A/mm}^2$. We can see that the flux created by the permanent magnets completes its loop in the magnetic bridge and only a small part passes through the air gap forming the remanent flux ϕ_0 . This means that with no excitation current, the machine is not magnetized despite the presence of permanent magnets, imitating therefore the behavior of a WF machine. The rectified remanent voltage for this machine is equal to only 13 V at 13000 rpm which is lower than the 16 V limit. This will lead to a small short-circuit current in case of fault as we will see later on. This machine has also a high flux variation ratio. Between $\delta_{exc} = 0 \text{ A/mm}^2$ and $\delta_{exc} = 12.5 \text{ A/mm}^2$, the flux varies from 1.45 mWb to 36.4 mWb with a ratio of 25.

Based on this analysis, we can conclude that the permanent magnets in the HEFSM do not form a 'real' excitation source as in classical hybrid machines. As Figure 9 shows, the PMs do not directly enhance the flux-linkage of the machine and are instead used to delay the saturation in the magnetic bridge (Nasr *et al.*, 2016). This will extend the efficient zone of the excitation coils in comparison with machines without permanent magnets, allowing better control and higher flux values. The HEFSM can be then described as a *hybrid-excited machine with low remanent flux*.

We can notice in Figure 9 that for current densities higher than 12.5 A/mm^2 , the flux starts to decrease. This characteristic is unusual for WF machines and is only specific for the HEFSM having each of its armature coils surrounding two stator

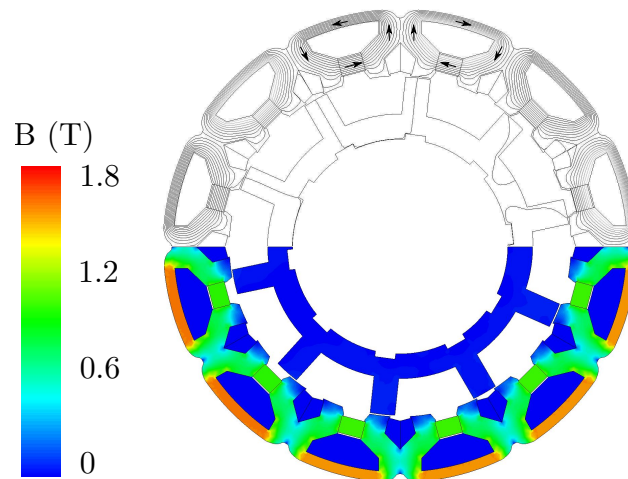


Figure 10. Flux lines and flux density patterns for $\delta_{exc} = 0 \text{ A/mm}^2$

teeth. Figure 11 shows the flux lines and the flux density patterns for the HEFSM for $\delta_{exc} = 20 \text{ A/mm}^2$. For each armature coil in d-axis position (the oriented coils in Figure 11), three main flux paths can be identified in the air-gap (1, 2 and 3). Between $\delta_{exc} = 0 \text{ A/mm}^2$ and $\delta_{exc} = 12.5 \text{ A/mm}^2$, the flux created by the field coil goes through path 1 forming the flux-linkage and mainly returns from path 3. This leads to the saturation of the stator and rotor teeth in zone 1 as well as the magnetic bridge (refer to the flux density pattern), limiting therefore the increase rate of the flux-linkage. For δ_{exc} higher than 12.5 A/mm^2 , the stator and rotor teeth in zone 3 start to saturate as well. This will create a secondary flux leakage path in zone 2. As shown in Figure 11 (flux lines), this leakage flux goes through the armature coil in the opposite direction of the main flux in zone 1, decreasing therefore the global flux-linkage.

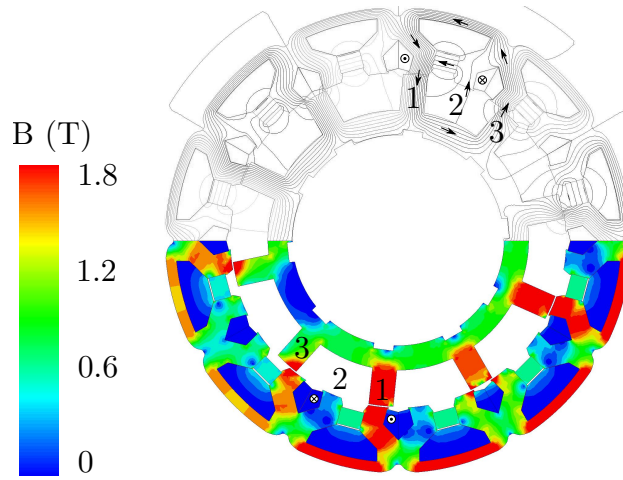


Figure 11. Flux lines and flux density patterns for $\delta_{exc} = 20 \text{ A/mm}^2$

3.2. DC alternator configuration

We will study in this section the performances of the HEFSM in a DC alternator configuration in which the machine is connected to a Diode Bridge Rectifier (DBR) feeding a 270 V DC bus. This configuration can be found in most of embedded systems like electric vehicles and aircraft with a DC electrical network. Figure 12 shows the schematic of such configuration with v the phase-to-neutral voltage, i the phase current, U_{DC} the DC bus voltage and i_{DC} the rectified current. In order to determine the generated electric power, a FE transient magnetic model (Ansys Maxwell, 2015) coupled with an external electric circuit has been used. Figure 13 shows the rectified current at 6000 rpm for several excitation current values. The DC generated power is

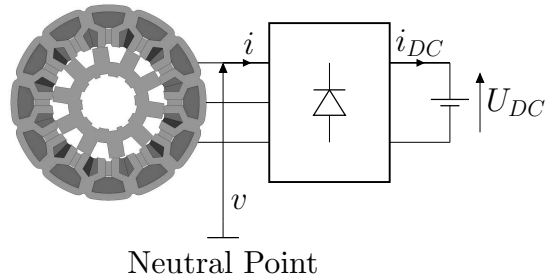


Figure 12. HEFSM associated with a DBR

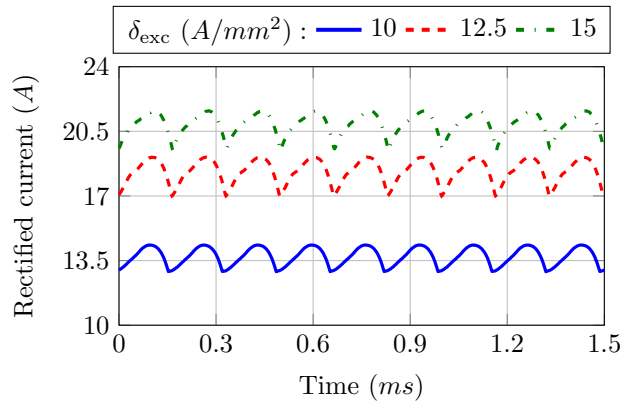


Figure 13. Rectified current at 6000 rpm

given in Figure 14 as a function of δ_{exc} for several rotational speeds. It is calculated as follows:

$$P_{DC} = \langle i_{DC} \rangle \cdot U_{DC} \tag{1}$$

with $\langle i_{DC} \rangle$ the mean value of the rectified current. At a fixed rotational speed and in the case of a DC alternator using DBR, the excitation current is the only parameter available to control the generated power. We can notice that at 6000 rpm the power is zero for δ_{exc} between 0 and 6 A/mm². In this zone, the back EMF generated by the machine does not exceed the phase voltage imposed by the DC bus, and thus no power can be generated. The RMS value V of the phase voltage is equal to :

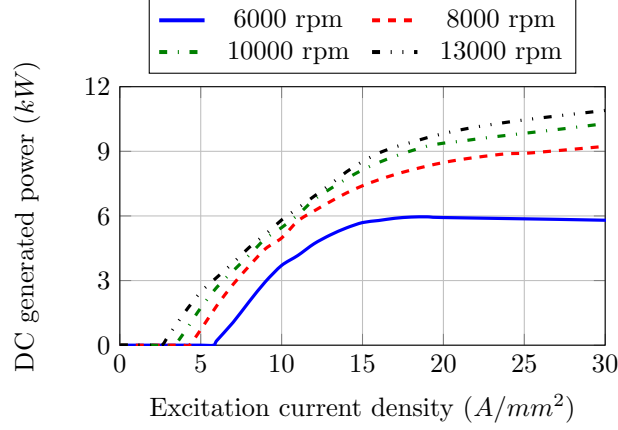


Figure 14. DC electromagnetic generated power

$$V = \frac{\sqrt{2}}{\pi} U_{DC} \quad (2)$$

For higher speeds, power generation begins at lower excitation current densities since the back EMF becomes higher.

In the case of embedded applications, the excitation current is controlled to generate a constant output power despite sudden changes in the rotational speed. It is also important for the machine to have high efficiency over a wide range of rotational speeds. We present in Figure 15, the evolution of the copper losses in the excitation winding P_{exc} at 100 °C, the core losses $P_{coreloss}$ and the efficiency η versus the rotational speed for a constant generated power of 3 kW. The efficiency is calculated by considering as well the copper losses in the armature windings P_{arm} which in this case are constant and equal to 158 W:

$$P_{arm} = 3 R_{ph} I^2 \quad (3)$$

with R_{ph} the phase resistance and I the RMS value of phase current. The efficiency is determined using :

$$\eta = \frac{P_{DC}}{P_{DC} + P_{exc} + P_{arm} + P_{coreloss}} \quad (4)$$

Core losses are calculated in post-processing using an integrated Bertotti model in the FE magnetic model. By increasing the rotational speed, a smaller excitation current is required to generate the desired power of 3 kW which justifies the decrease of the

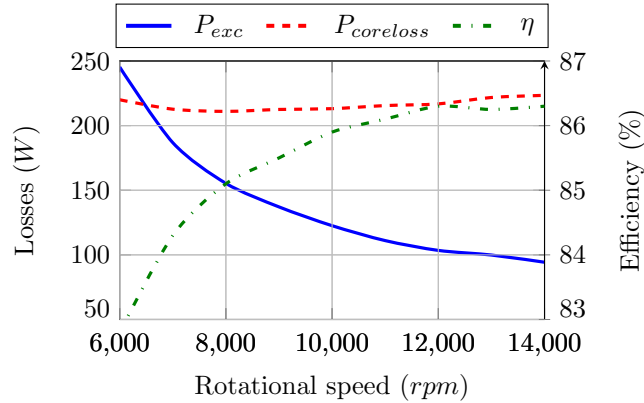


Figure 15. Excitation copper losses, core losses and efficiency versus rotational speed for a constant output power of 3 kW

losses in the excitation. As for core losses, they are almost constant over the entire speed range of 6000 - 14000 rpm with 220 W. The efficiency varies from 83 % to 86 % with the maximum reached at 12000 rpm.

3.3. Motor mode

The machine presented in this paper is initially designed to work as a generator. However, in some applications, it is required that the machine also operates in motor mode for a certain period of time. This starter-generator operation is increasingly demanded in embedded applications considering its advantages in terms of weight and volume (Chedot *et al.*, 2007; Liu *et al.*, 2010; Abdelhafez, Forsyth, 2009). Figure 16 shows the instantaneous electromagnetic torque generated by the machine for several armature current densities (δ_{exc} is fixed at 8 A/mm^2). Only quadrature-axis armature current has been considered because the reluctance torque in the HEFSM is negligible. In fact, despite the salient shape of its rotor, the HEFSM has a nearly constant phase inductance during an electrical period unlike the switched reluctance machine. Figure 17 shows the mean value of the electromagnetic torque versus δ_{arm} for several excitation current density. Once again, we can notice the importance of the hybrid excitation in controlling the generated torque. By increasing the excitation current from 2 A/mm^2 to 10 A/mm^2 , the variation rate of the torque (the slope) using the armature current increases from $0.15 \text{ N.m/(A/mm}^2)$ to $0.52 \text{ N.m/(A/mm}^2)$, improving therefore the controllability of the machine.

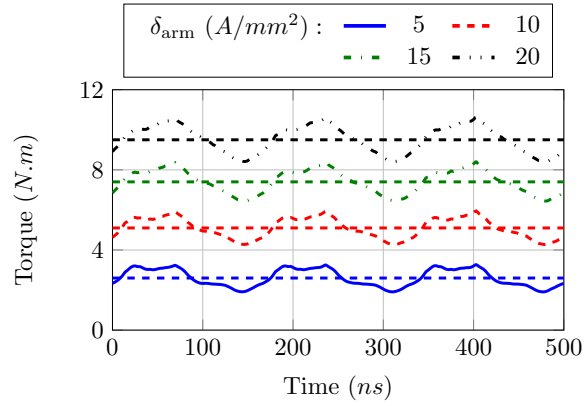


Figure 16. Electromagnetic torque for $\delta_{exc} = 8 \text{ A/mm}^2$

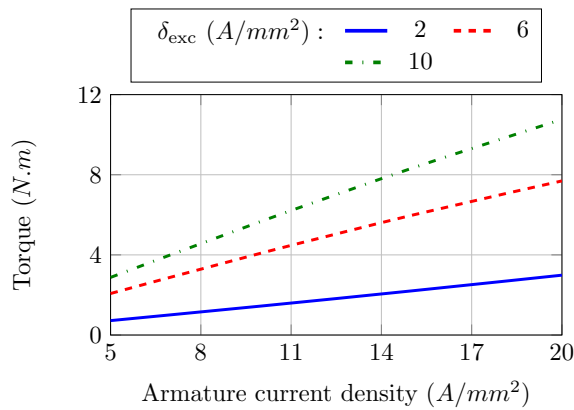


Figure 17. Electromagnetic torque versus δ_{arm}

4. Short-circuit current limitation : Impact of the geometric and magnetic parameters of the HEFSM on its performances

We will examine in this section the impact of the magnetic bridge width W_{bridge} (Figure 18) and the remanent flux density B_r of the permanent magnets on the overall performances of the HEFSM especially on its short-circuit current limitation characteristic. We will consider the case of a DC short-circuit at the DBR output as shown in Figure 19 (the short-circuit occurs when switch 1 is closed).

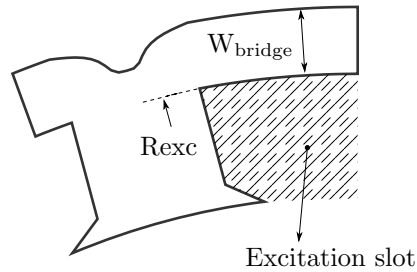


Figure 18. Geometric parameters in the HEFSM

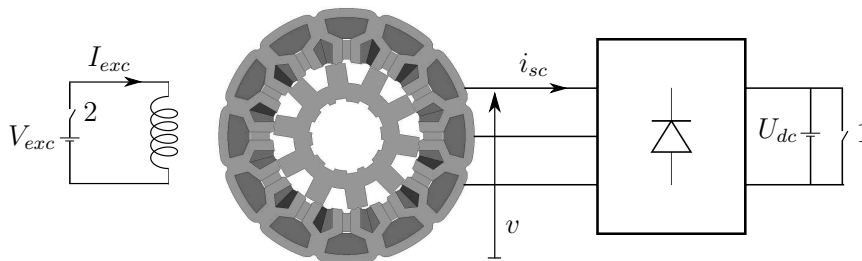


Figure 19. DC short-circuit

The phase short-circuit current is given in Figure 20 versus the excitation current density δ_{exc} . We can notice that by cutting off the excitation current ($\delta_{exc} = 0 \text{ A/mm}^2$), the fault current I_{sc0} becomes very small and is limited to only 0.75 Arms. This characteristic of the HEFSM is very important for safety as the fault current can cause no damage to the machine, unlike classical hybrid-excited machines.

Figure 21 shows the phase current response to a scenario with the following three stages :

- At $t < 5 \text{ ms}$: The machine was generating 3 kW at 6000 rpm (switch 1 open, switch 2 closed).
- At $t = 5 \text{ ms}$: A short-circuit at the DBR output occurs (switch 1 closed, switch 2 closed).
- At $t = 20 \text{ ms}$: The excitation source has been cut-off (switch 1 closed, switch 2 opened).

When the short-circuit occurs at $t = 5 \text{ ms}$, we can notice that the phase current get into a transient state for a very short period (5 ms) and reaches a maximum amplitude of

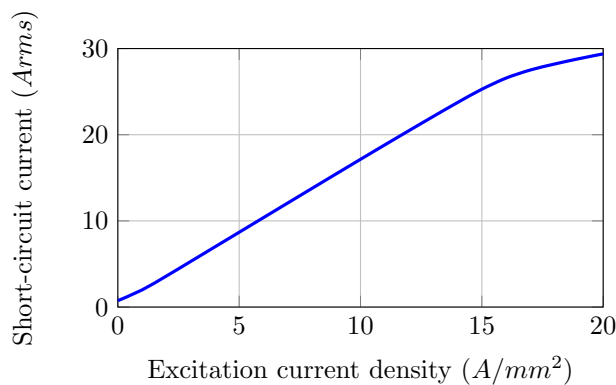


Figure 20. Phase short-circuit current versus δ_{exc}

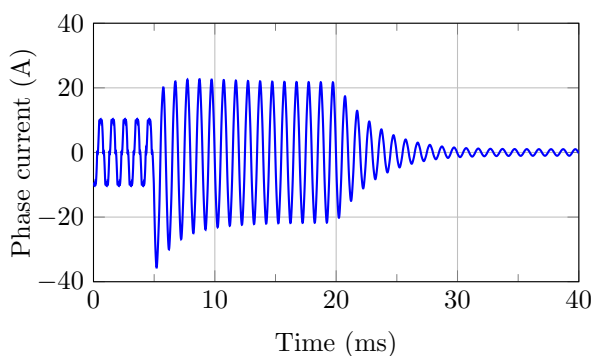


Figure 21. Phase current response to a short-circuit

38 A. However, once the steady state is reached (around $t = 10$ ms), the short-circuit current is only 2 times bigger than the nominal current at 3 kW (between $t = 0$ ms and $t = 5$ ms). At 20 ms, the excitation source has been cut-off (voltage step). The phase current response is of a first order system with a time constant of approximately 3 ms. This result clearly shows the safety characteristics of the HEFSM : the short-circuit current is relatively small compared to the phase current in normal condition and can be quickly limited by cutting-off the excitation source despite the presence of permanent magnets.

4.1. Magnetic bridge width (W_{bridge})

We will study in this section the impact of the magnetic bridge width W_{bridge} on the performances of the HEFSM including its phase short-circuit current I_{sc0} at $\delta_{exc} = 0 \text{ A/mm}^2$. In order to change W_{bridge} , we have chosen to change the radius of the excitation slot R_{exc} (Figure 18) while keeping fixed the external diameter of the machine. By increasing R_{exc} , W_{bridge} gets smaller and vice versa. Figure 22 shows the evolution of I_{sc0} versus W_{bridge} . This figure shows a direct link between the two. The short-circuit current gets bigger when decreasing the width of the magnetic bridge. In fact, if we go back to Figure 10, we can see that the magnetic bridge is already saturated at $\delta_{exc} = 0 \text{ A/mm}^2$ with a flux density of 1.6 T. Decreasing the width of the magnetic bridge will increase the saturation even more which will lead to a higher remanent flux-linkage ϕ_0 as shows Figure 23, and therefore a bigger short-circuit current.

Based on these results, one can say that increasing W_{bridge} would lead to a *safer* machine. But by doing that, the slot dedicated to the excitation coils (Figure 18) will get smaller which will lead to higher current densities in load conditions. The change of W_{bridge} has also a big impact on the electromagnetic performances of the machine. Figure 24 shows the DC generated power at 6000 rpm for several values of W_{bridge} . We can notice that increasing W_{bridge} allows us to reach higher power values. This is mainly due to the increased efficiency of the excitation coils with a wider magnetic bridge. However, with smaller excitation slots¹, the current density needed gets also higher which leads to more losses. This outcome can also be seen for the nominal

1. An increase in W_{bridge} will lead to smaller excitation slots.

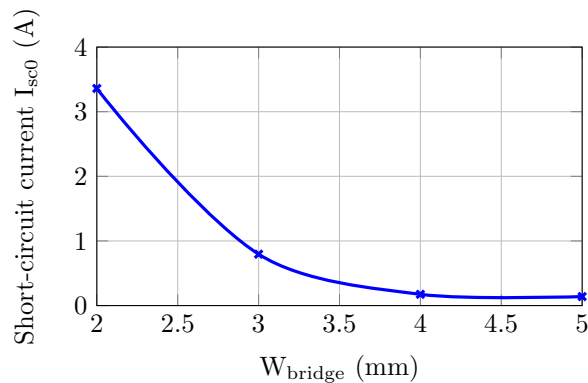


Figure 22. Evolution of I_{sc0} ($\delta_{exc} = 0 \text{ A/mm}^2$) versus W_{bridge}

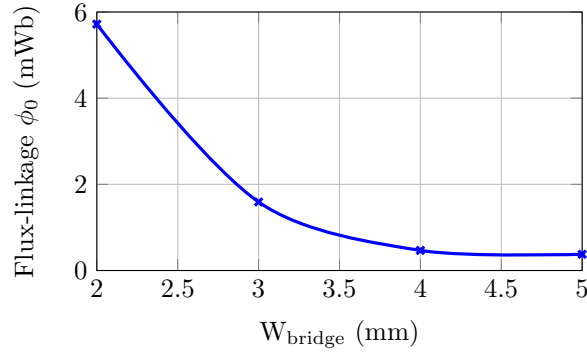


Figure 23. Evolution of the remanent flux-linkage ϕ_0 ($\delta_{exc} = 0 \text{ A/mm}^2$) versus W_{bridge}

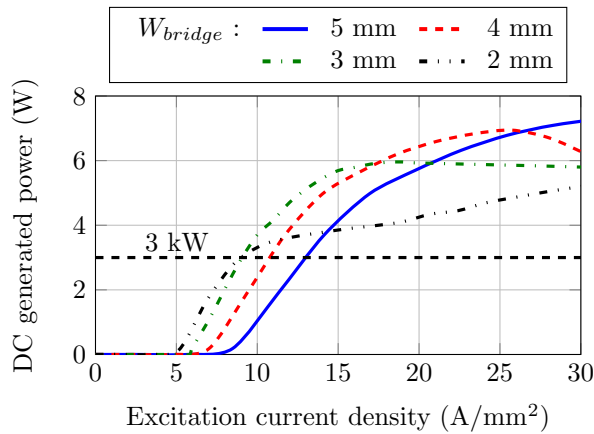


Figure 24. Impact of W_{bridge} on the DC generated power at 6000 rpm

power of 3 kW. For $W_{bridge} = 3 \text{ mm}$ which is the initial value, the machine reaches its nominal power for $\delta_{exc} = 8 \text{ A/mm}^2$. By increasing W_{bridge} to 5 mm, the same power is reached for $\delta_{exc} = 13 \text{ A/mm}^2$. These facts show the importance of the design phase of the HEFSM in order to find the right balance between safety and high performances. We can also see in Figure 24 that the machine starts generating at different excitation current densities depending on the value of W_{bridge} . The initial design ($W_{bridge} = 3 \text{ mm}$) has its starting point at $\delta_{exc} = 6 \text{ A/mm}^2$. By increasing

W_{bridge} to 5 mm, the power production starts further at $\delta_{exc} = 8 A/mm^2$. This can be explained by looking at Figure 25. We can notice that the flux-linkage gets smaller at $\delta_{exc} = 6 A/mm^2$ when increasing W_{bridge} . This means that the back-EMF gets also smaller and a higher excitation current density is needed to start generating power on the DC bus.

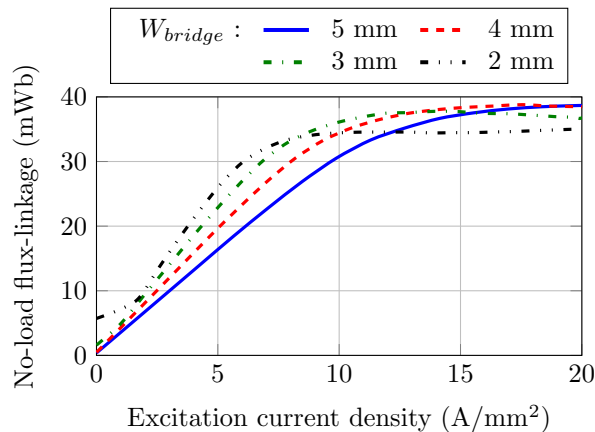


Figure 25. Impact of W_{bridge} on the no-load flux-linkage

4.2. PM remanent flux density (B_r)

Figure 26 shows the evolution of the short-circuit current I_{sc0} for $\delta_{exc} = 0 A/mm^2$ versus the PMs remanent flux density B_r . By decreasing B_r , I_{sc0} decreases too. Between 1.2 T and 0.8 T, I_{sc0} is reduced from 2.04 A to 0.18 A (-91 %). By decreasing B_r furthermore from 0.8 T to 0.4 T, I_{sc0} decreases by a smaller rate of -58 % (0.18 A to 0.075 A). Concerning the DC generated power, Figure 27 shows that B_r is a very influential parameter. At first, it allows to reach much higher power. At $\delta_{exc} = 20 A/mm^2$ for example, using permanent magnets with a remanent flux density of 1.2 T instead of 0.4 T can increase the generated power from 2.5 kW to 6.8 kW. On the other hand, increasing B_r allows to reach the nominal power of 3 kW with smaller excitation current densities helping increase the efficiency. In comparison with Figure 24, we can notice in Figure 27 that the power generation starting point does not change with B_r . In fact, if we look at Figure 28, we can see that the flux-linkage at $\delta_{exc} = 6 A/mm^2$ is almost the same unlike the case when changing W_{bridge} .

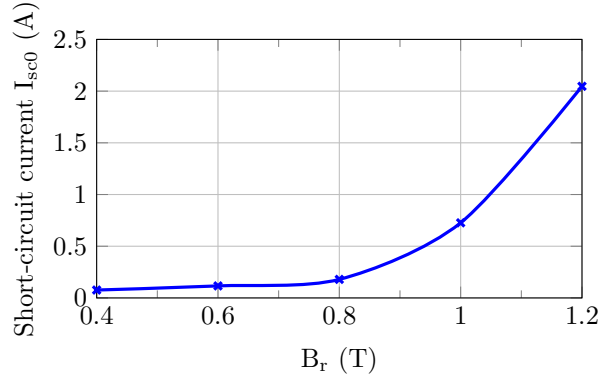


Figure 26. Evolution of I_{sc0} ($\delta_{exc} = 0 \text{ A/mm}^2$) versus B_r for $W_{bridge} = 3 \text{ mm}$

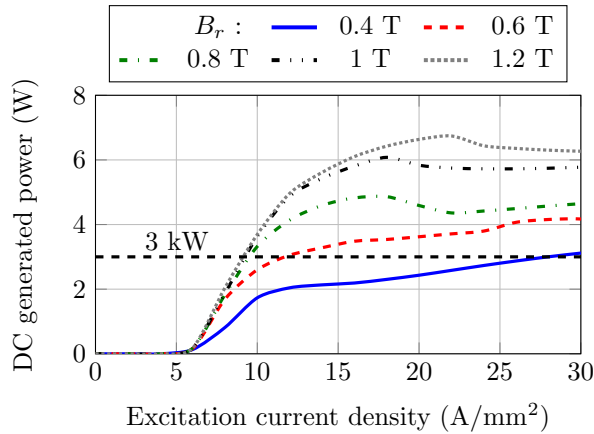


Figure 27. Impact of B_r on the DC generated power at 6000 rpm for $W_{bridge} = 3 \text{ mm}$

These two sensibility studies have shown that both W_{bridge} and B_r have somehow a similar impact on I_{sc0} . Increasing W_{bridge} and decreasing B_r have led to smaller values of the short-circuit current at $\delta_{exc} = 0 \text{ A/mm}^2$. However, we have also seen that these two parameters affect differently the behavior of the machine in generator mode. Increasing B_r will help reaching higher power with better efficiency at nominal power. As for W_{bridge} , it is not that obvious. Increasing W_{bridge} will allow reaching higher power but will also increase the excitation current densities and reduce the

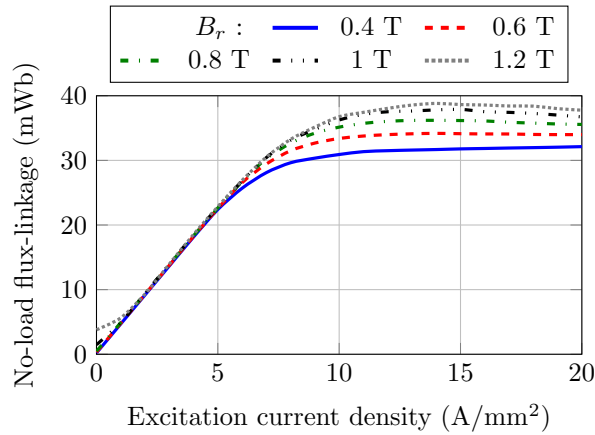


Figure 28. Impact of B_r on the no-load flux-linkage for $W_{bridge} = 3 \text{ mm}$

efficiency of the machine. Many other geometric parameters could have been added to this study. However, in that case, a multi-dimensional parametric study is required because of the high interdependency of the parameters due to the complex structure of the stator.

5. Conclusion

Hybrid-excited machines combine the advantages of permanent magnet machines and wound-field machines : high power density, high efficiency and flux regulation capability. These characteristics make the hybrid-excited machine the first choice for power systems in many embedded applications. However, these machines are avoided in critical applications like aircraft power generation due to safety concerns. In fact, in case of a fault, the uncontrolled high remanent voltage can cause a high short-circuit current that can damage the whole system. That's why wound-field machines are usually used instead because of their demagnetizing capability. The Hybrid-Excited Flux Switching Machine (HEFSM) presented in this paper has the same characteristics as the wound-field machine. Despite having permanent magnets, the HEFSM can be demagnetized by simply cutting off the excitation current. In fact, when no excitation current is used, the flux created by the permanent magnets is short-circuited by the magnetic bridge in the stator which means that the remanent flux-linkage can be very small. The design presented in this paper has a rectified remanent back-EMF of only 13 V at 13000 rpm which is in the safety limits for aircraft power systems. This characteristic has been proved very important for limiting the short-circuit current in case of a fault. Despite this low remanent back-EMF, it has been shown that the permanent magnets improve the performances of the machine and allow to reach higher flux-

linkage. Sensibility studies have also shown that these performances can be further improved by changing the width of the magnetic bridge and the remanent flux-density of the permanent magnets . However, in order to have a good balance between safety and high performance, these parameters must be carefully chosen and optimal design techniques must be used.

References

- Abdelhafez A. A., Forsyth A. J. (2009, May). A review of more-electric aircraft. In *13th international conference on aerospace science and aviation technology*.
- Amara Y., Vido L., Gabsi M., Hoang E., Ahmed A. H. B., Lecrivain M. (2009, Jun). Hybrid excitation synchronous machines: Energy-efficient solution for vehicles propulsion. *IEEE Transactions on Vehicular Technology*, Vol. 58, No. 5, pp. 2137-2149.
- Ammar A., Gillon F., Brochet P. (2012). The double excitation: A solution to improve energetic performances of high power synchronous machines. *Journal of Energy and Power Engineering*, Vol. 6, pp. 719 - 724.
- Avery C. R., Burrow S. G., Mellor P. H. (2007, Sept). Electrical generation and distribution for the more electric aircraft. In *2007 42nd international universities power engineering conference*, p. 1007-1012.
- Cai W. (2004, Oct). Comparison and review of electric machines for integrated starter alternator applications. In *Conference record of the 2004 IEEE industry applications conference, 2004. 39th IAS annual meeting.*, Vol. 1, p. 393.
- Chau K. T., Chan C. C. (2007, April). Emerging energy-efficient technologies for hybrid electric vehicles. *Proceedings of the IEEE*, Vol. 95, No. 4, pp. 821-835.
- Chedot L., Friedrich G., Biedinger J. M., Macret P. (2007, March). Integrated starter generator: The need for an optimal design and control approach. application to a permanent magnet machine. *IEEE Transactions on Industry Applications*, Vol. 43, No. 2, pp. 551-559.
- Friedrich G., Girardin A. (2009, July). Integrated starter generator. *IEEE Industry Applications Magazine*, Vol. 15, No. 4, pp. 26-34.
- Hlioui S., Amara Y., Hoang E., Gabsi M. (2013, March). Overview of hybrid excitation synchronous machines technology. In *2013 international conference on electrical engineering and software applications*, p. 1-10.
- Hoang E., Ahmed H. B., Lucidarme J. (1997). Switching flux permanent magnet polyphased synchronous machines, trondheim, norway. *European Conference on Power Electronics and Applications*.
- Hoang E., Gabsi M., Lecrivain M., Multon B. (2000). Influence of magnetic losses on maximum power limits of synchronous permanent magnet drives in flux-weakening mode. In *Conference record of the 2000 IEEE industry applications conference. thirty-fifth IAS annual meeting and world conference on industrial applications of electrical energy (cat. no.00ch37129)*, Vol. 1, p. 299-303 vol.1.
- Hoang E., Lecrivain M., Gabsi M. (2007). *Flux-switching dual excitation electrical machine* No. US 7868506 B2.

- Laskaris K. I., Kladas A. G. (2010, Jan). Internal permanent magnet motor design for electric vehicle drive. *IEEE Transactions on Industrial Electronics*, Vol. 57, No. 1, pp. 138-145.
- Leonardi F., McCleer P. J., Lipo T. (1997, June). The dspm: An ac permanent magnet traction motor with true field weakening. In *2nd international conference on "all electric combat vehicle"*. Detroit MI.
- Liu C., Chau K. T., Jiang J. Z. (2010, Dec). A permanent-magnet hybrid brushless integrated starter-generator for hybrid electric vehicles. *IEEE Transactions on Industrial Electronics*, Vol. 57, No. 12, pp. 4055-4064.
- Nasr A., Gabsi M., Hlioui S. (2016, Oct). Hybrid-excited flux-switching machine for dc alternator applications. new design for fault short-circuit current limitation. In *2016 international conference on electrical sciences and technologies in maghreb (cistem)*, p. 1-7.
- Nasr A., Hlioui S., Gabsi M., Mairie M., Lalevee D. (2017a, Dec). Design optimization of a hybrid-excited flux-switching machine for aircraft-safe dc power generation using a diode bridge rectifier. *IEEE Transactions on Industrial Electronics*, Vol. 64, No. 12, pp. 9896-9904.
- Nasr A., Hlioui S., Gabsi M., Mairie M., Lalevee D. (2017b, May). Experimental investigation of a doubly-excited flux-switching machine for aircraft dc power generation. In *2017 IEEE international electric machines and drives conference (iemdc)*, p. 1-7.
- Owen R. L., Zhu Z. Q., Jewell G. W. (2010, June). Hybrid-excited flux-switching permanent-magnet machines with iron flux bridges. *IEEE Transactions on Magnetics*, Vol. 46, No. 6, pp. 1726-1729.
- Raimondi G. M., Sawata T., Holme M., Barton A., White G., Coles J. *et al.* (2002, June). Aircraft embedded generation systems. In *2002 international conference on power electronics, machines and drives (conf. publ. no. 487)*, p. 217-222.
- Ansys Maxwell. (2015, Release 16.2). Ansys ®, *electromagnetics suite*.
- Wang Y., Deng Z. (2012a, Sept). Comparison of hybrid excitation topologies for flux-switching machines. *IEEE Transactions on Magnetics*, Vol. 48, No. 9, pp. 2518-2527.
- Wang Y., Deng Z. (2012b, Dec). Hybrid excitation topologies and control strategies of stator permanent magnet machines for dc power system. *IEEE Transactions on Industrial Electronics*, Vol. 59, No. 12, pp. 4601-4616.
- Zhang B., Qu R., Xu W., Li J. (2015, Nov). A permanent magnet traction machine with wide high efficiency range for ev application. In *Iecon 2015 - 41st annual conference of the IEEE industrial electronics society*, p. 000457-000463.
- Zhu X., Cheng M. (2005, Sept). A novel stator hybrid excited doubly salient permanent magnet brushless machine for electric vehicles. In *2005 international conference on electrical machines and systems*, Vol. 1, p. 412-415 Vol. 1.